Timing of Deformation along the Iron Springs Thrust, Southern Sevier Fold-and-Thrust Belt, Utah: Evidence for an Extensive Thrusting Event in the mid-Cretaceous

J. Daniel Quick

John Patrick Hogan
Missouri University of Science and Technology, jhogan@mst.edu

Michael Wizevich

Jonathan Obrist-Farner
Missouri University of Science and Technology, obristj@mst.edu

et. al. For a complete list of authors, see https://scholarsmine.mst.edu/geosci_geo_peteng_facwork/1839

Recommended Citation

J. D. Quick et al., "Timing of Deformation along the Iron Springs Thrust, Southern Sevier Fold-and-Thrust Belt, Utah: Evidence for an Extensive Thrusting Event in the mid-Cretaceous," *Rocky Mountain Geology*, vol. 55, no. 2, pp. 75-89, University of Wyoming, Dec 2020.
The definitive version is available at https://doi.org/10.24872/rmgjournal.55.2.75

Timing of deformation along the Iron Springs thrust, southern Sevier fold-and-thrust belt, Utah: Evidence for an extensive thrusting event in the mid-Cretaceous

J. Daniel Quick[1], John P. Hogan[1]*, Michael Wizevich[2], Jonathan Obrist-Farner[1], and James L. Crowley[3]

[1]*Department of Geosciences, Geological Engineering, and Petroleum Engineering, Missouri University of Science and Technology, 129 McNutt Hall, 1400 N. Bishop, Rolla, MO 65409*

[2]*Department of Geological Sciences, Central Connecticut State University, Copernicus Hall, Room 506, 1615 Stanley St., New Britain, CT 06050*

[3]*Department of Geosciences, Boise State University, Environmental Research Building 1160, 1910 University Dr., MS 1535, Boise, ID 83725*

**Correspondence should be addressed to: jhogan@mst.edu*

ABSTRACT

The temporal and spatial distribution of strain associated with the Sevier orogeny in western North America is significantly different in the southern end of the belt, at the latitude of Las Vegas, Nevada, than farther to the north at the latitude of Salt Lake City, Utah. Reasons for these differences have been speculative as a lack of temporal constraints on thrusting in the intervening region hindered along-strike correlation across the belt. We determined a crystallization age of 100.18 ± 0.04 Ma for zircons extracted from a recently recognized dacite lapilli ash-fall tuff near the base of the synorogenic Iron Springs Formation. We propose the name "Three Peaks Tuff Member" for this unit, and identify a type stratigraphic section on the western flank of the "Three Peaks," a topographic landmark in Iron County, Utah. Field relationships and this age constrain movement on the Iron Springs thrust and the end of the sub-Cretaceous unconformity in the critical intervening area to latest Albian/earliest Cenomanian. Movement on the Iron Springs thrust was synchronous with movement on multiple Sevier thrusts at ~100 Ma, indicating that the mid-Cretaceous was a period of extensive thrust-fault movement. This mid-Cretaceous thrusting event coincided with a period of global plate reorganization and increased convergence, and hence an increased subduction rate for the Farallon Plate beneath North America. The accelerated subduction contributed to a Cordilleran arc flare-up event and steepening of the orogenic wedge, which triggered widespread thrusting across the retroarc Sevier deformation belts. Additionally, based on temporal constraints and the strong spatial connection of mid-Cretaceous thrusts to lineaments interpreted as pre-orogenic transform faults, we suggest that temporal and spatial variations along the strike of the orogenic belt reflect tectonic inheritance of basement structures associated with the edge of the rifted Precambrian craton.

KEY WORDS: Cordilleran orogeny, dacite lapilli ash-fall tuff, Iron Springs thrust, magma flare-up, structural inheritance, sub-Cretaceous unconformity, Three Peaks Tuff Member.

INTRODUCTION

The Sevier orogenic system is an important component of the Cordilleran orogeny that affected the western North American Cordillera beginning in the Middle Jurassic (~165 Ma) to the early Eocene (~50 Ma) (Yonkee and Weil, 2015; Herring and Greene, 2016; Fig. 1 this paper). Deformation during this time, attributed to plate convergence, subduction of oceanic lithosphere, and accretion of various terranes along the edge of western North America, telescoped the antecedent passive margin along several prominent, east-directed thrusts, resulting in at least 350 km of shortening at the latitude of central Utah (DeCelles, 2004; Herring and Greene, 2016). Crustal shortening associated with the Sevier orogeny produced several roughly N–S-trending thrust belts, fold belts, and fold-and-thrust belts extending from the hinterland in western Nevada to the foreland in Utah (Fig. 1). We use the term "fold-and-thrust belt" *sensu lato* for these domains as these thrust belts include folds (e.g., see Herring and

Received 31 August 2020 • Revised submitted 9 November 2020 • Accepted 12 November 2020 • Published online December 2020

Greene, 2016, their fig. 3, p. 137). The exception to our application of fold-and-thrust belt is the eastern Nevada fold belt, which is characterized by a notable absence of regional-scale thrust faults (Long, 2015). The temporal and spatial evolution of the fold-and-thrust deformation associated with the Sevier orogeny varies along strike. Near Las Vegas, Nevada, thrust-fault propagation in the Sevier fold-and-thrust belt is restricted in time (ca. 50 m.y.) and space (< 100 km) where it is defined by the Wheeler Pass thrust (160–140 Ma; Giallorenzo et al., 2018) to the west and the Keystone thrust (99 Ma; Fleck and Carr, 1990) on the eastern edge. At this same latitude is the central Nevada fold-and-thrust belt, which developed, to an extent, synchronously with the Sevier fold-and-thrust belt (Di Fiori et al., 2020) and is considered part of the Sevier orogeny. At the latitude of Salt Lake City, Utah, the zone of fold-and-thrust belt deformation widens considerably (~500 km), and includes several fold-and-thrust belts that were active over a prolonged period (ca. 100 m.y.; Herring and Greene, 2016). At this latitude, the westernmost edge is defined by the Luning-Fencemaker fold-and-thrust belt of central Nevada, potentially related to the closure of a Jurassic back-arc basin (~165–150 Ma; Wyld et al., 2003), and the eastern edge by the Hogsback thrust of western Wyoming, which represents the eastern leading edge of the Sevier fold-and-thrust belt (~56 Ma; DeCelles, 1994). Some workers consider the Luning-Fencemaker fold-and-thrust belt as part of the Sevier orogeny (e.g., Herring and Greene, 2016), whereas others (e.g., Wyld et al., 2003) suggest that it is unrelated to the Sevier fold-and-thrust belt. Even if the Luning-Fencemaker fold-and-thrust belt is excluded from consideration, significant along-strike variation exists in the map view width of fold-and-thrust belt deformation that define the Sevier orogeny. This extreme along-strike variation in map width exists despite the fact that the southernmost portion of Sevier fold-and-thrust belt deformation (i.e., southern Nevada to southwestern Utah) resides completely in the Basin and Range Province, characterized by Cenozoic extension, whereas the northern portion of the deformation belt (i.e., central and northern Utah–western Wyoming, see Fig. 1) only partially resides within the Basin and Range Province (Yonkee and Weil, 2015).

The sinuous trace of the leading edge of deformation belts, defined by multiple recesses and salients, is an intrinsic feature of many collisional orogens (e.g., Appalachian, Lesser Himalaya, Ouachita, and Zagros) including the Sevier fold-and-thrust belt of the Cordilleran orogeny (Fig. 1). Along-strike variation in the shape of orogens has been attributed to "tectonic inheritance," where the form of the orogen mirrors the form of the previous rifted continental margin (e.g., Thomas, 1977, 2005). Additionally, fold-and-thrust belt development may be controlled by variation in stratigraphy (e.g., Chapman and DeCelles, 2015) and sediment thickness (e.g., Paulsen and Marshak, 1999). Evaluating the role of tectonic inheritance, stratigraphy, and tectonic models for thrusting in the evolution of the Sevier orogeny requires temporal correlation of spatially distributed fold-and-thrust belts in the north (e.g., western Utah thrust belt of Greene, 2014) to the narrower zone of fold-and-thrust belts in the south. Considerable uncertainty in the timing of the eastward propagation of the leading edge along the entire strike of the Sevier fold-and-thrust belt has limited advancement of the understanding of the extent to which tectonic inheritance, linked vs. independent thrusts, and broader plate-tectonic processes had on the evolution of the Sevier fold-and-thrust belt.

We present here the first complete description and high-precision zircon U–Pb geochronology of a previously unreported volcanic ash unit near the base of the synorogenic Cretaceous Iron Springs Formation in southwest Utah. We propose the name "Three Peaks Tuff Member of the Iron Springs Formation," and identify the type section. We interpret the base of the Iron Springs Formation to include the Marshall Creek breccia, which originated as debris flows proximal to the Iron Springs thrust. Our findings place the eastern leading edge of the Sevier orogenic belt, in the critical intervening area, significantly farther east (~50 km; e.g., see Long, 2015, his fig. 6, p. 415) at an earlier point in time (100 Ma) than previously thought (Herring and Greene, 2016, their fig. 2, p. 136; Yonkee et al., 2019). Our results, combined with multiple recently published dates for thrusting (e.g., Pujols et al., 2020), provide evidence for a regionally extensive, large-scale, mid-Cretaceous thrusting event, which is temporally correlative to the mid-Cretaceous magmatic flare-up identified by Ducea et al., (2015). We place these results in a larger regional context to discuss the role of tectonic inheritance and plate-tectonic processes in the evolution of the Sevier fold-and-thrust belt.

GEOLOGIC SETTING

The Iron Springs thrust (IST, Fig. 1) is exposed about 16 km to the west of Cedar City and the town of Kanarra, where the Kanarra fold and associated thrusts (e.g., Taylor Creek and Kanarra Creek thrusts) mark the easternmost limit of Sevier-style deformation at this latitude (Chandonia et al., 2018). The Iron Springs thrust appears to have accommodated about 5.6 km of shortening, based on local seismic data collected within the vicinity of the Three Peaks (Van Kooten, 1988). In addition to the Taylor Creek thrust, several newly recognized thrusts (e.g., Spring Creek and Kanarra Creek thrusts, see Chandonia et al., 2018) associated with the Kanarra fold accommodated several kilometers of shortening. The proximity of the Iron Springs thrust to

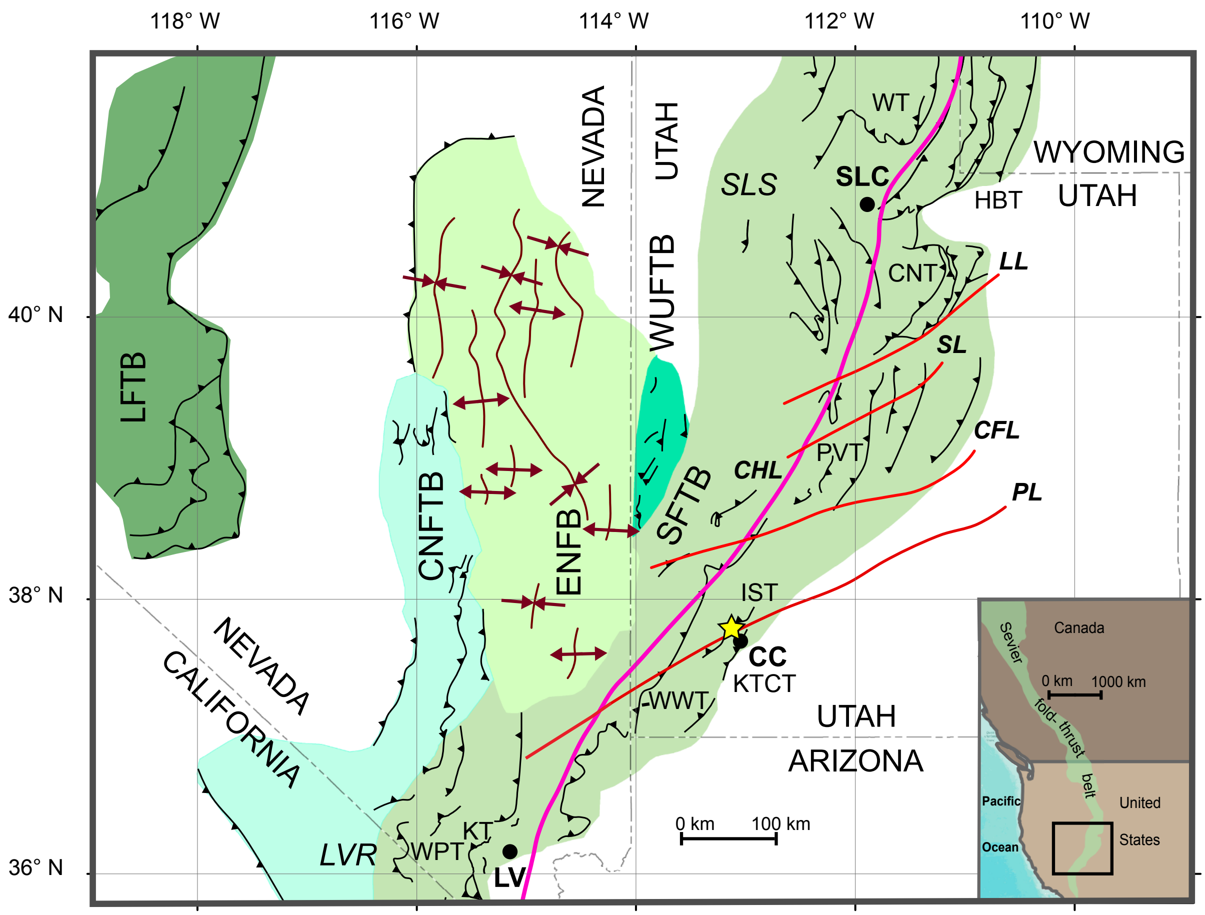

Figure 1. Location map showing the individual deformation belts and major thrust faults that comprise the Sevier orogeny. Also shown are significant basement structures (i.e., hingeline and lineaments) that affected eastward propagation of the Sevier deformation front leading to development of the newly named Las Vegas recess and the Salt Lake salient. Location of the Three Peaks is marked by the yellow star. CC = Cedar City; CFL = Cove Fort lineament; CHL = Cordilleran hingeline (purple); CNFTB = central Nevada fold-and-thrust belt; CNT = Charleston-Nebo thrust; ENFB = eastern Nevada fold belt; HBT = Hogsback thrust; IST = Iron Springs thrust; KT = Keystone thrust; KTCT = Kanarra fold and Kanarra-Taylor Creek thrust system; LFTB = Luning-Fencemaker fold-and-thrust belt; LL = Leamington lineament; LV = Las Vegas; LVR = Las Vegas recess; PL = Paragonah lineaments (lineament traces in red); PVT = Pavant thrust; SFTB = Sevier fold-and-thrust belt; SL = Scipio lineament; SLC = Salt Lake City; SLS = Salt Lake salient; WPT = Wheeler Pass thrust; WT = Willard thrust; WUFTB = western Utah fold-and-thrust belt; WWT = Wah Wah thrust. Compiled from Stokes et al. (1963), Picha and Gibson (1985), Willis (1999), Wyld et al., (2003), Page et al. (2005), Long (2015), Yonkee and Weil (2015), Herring and Greene (2016), and Giallorenzo et al. (2018).

these leading-edge structures, even without palinspastic restoration of basin-and-range extension, indicates the possibility of a shared décollement (e.g., Herring and Greene, 2016), and it could be considered part of the same "thrust system."

West of the Iron Springs thrust is the Wah Wah thrust (Willis, 1999). The Wah Wah thrust system accommodated a minimum of 38 km of total shortening (Friedrich and Bartley, 2003). The timing of the emplacement of the Wah Wah thrust is poorly constrained. Some authors (e.g., Willis, 1999) proposed it is the along-strike equivalent of the Late Jurassic–Early Cretaceous Canyon Range thrust exposed to the north (DeCelles and Coogan, 2006). The Iron Springs Formation at Three Peaks contains quartzite clasts eroded from the hanging wall of the Wah Wah thrust (Fillmore, 1991). Therefore, based on the stratigraphic relationships at Three Peaks (see below), the Wah Wah thrust was emplaced prior to the Iron Springs thrust, and these thrusts together represent a forward-breaking, eastward-propagating sequence. Total shortening along a 'thrust system,' which could include the Iron Springs thrust and the Kanarra and Taylor Creek thrusts associated with the Kanarra fold (Fig. 1), was significantly greater than 5.6 km, but basin-and-range overprinting complicates palinspastic reconstruction.

STRATIGRAPHIC RELATIONSHIPS AT THREE PEAKS

The "Three Peaks" (Figs. 2 and 3) is a topographic landmark just west of Cedar City. They are a series of rugged hills cored by Miocene quartz monzonite laccoliths (Mackin and Rowley, 1976; Barker, 1995; Knudsen and Biek, 2014). Cropping out on the western flank of the laccolith are the Co-op Creek Limestone Member and the Crystal Creek Member of the Jurassic Carmel Formation (Fig. 2). These units are disconformably overlain by the synorogenic Cretaceous Marshall Creek breccia, which is, in turn, conformably overlain by and interfingers with synorogenic clastic rocks of the Iron Springs Formation (Fig. 4). Along strike to the south, the sedimentary section is folded and overturned in the footwall of the Iron Springs thrust (Mackin et al., 1976; Knudsen and Biek, 2014; Fig. 2 this paper).

Two stratigraphic sections, the 'Central Creek' and 'Shooting Range' transects, were measured at Three Peaks (Figs. 2–4). The sections begin at the top of the shallow-marine Co-op Creek Limestone Member, a light gray to blackish gray, algal-laminated, lime mudstone, and they extend only 10s of meters into the Iron Springs Formation, which is locally more than 900 m thick (Mackin, 1947; Mackin et al., 1976). The Co-op Creek Limestone is overlain by the Crystal Creek Member. At Three Peaks, the Crystal Creek Member consists of channelized fluvial deposits of cream white sandstone and reddish brown to maroon mudstone.

Here, the base of the Cretaceous sedimentary section is marked by the appearance of the distinctive Marshall Creek breccia, which is confined to the western flank of Three Peaks (Mackin, 1947) and disconformably overlies the Crystal Creek Member of the Carmel Formation (Figs. 2 and 4). The Marshall Creek breccia is composed primarily of angular, lime mudstone pebbles to boulders (> 1.5 m across), supported by a brown lime-silt matrix (Fig. 5). Scarce sub- to well-rounded limestone clasts and sparse well-rounded quartzite pebbles and cobbles are also part of this unit (Fig. 5). Limestone clasts from the Marshall Creek breccia conspicuously resemble the limestone of the Co-op Creek Limestone Member of the Carmel Formation. Locally, the Marshall Creek breccia grades upward into, and interfingers with, a basal quartzite conglomerate of the Iron Springs Formation over a stratigraphic interval of up to ~18 m (Fig. 4). Above this contact, the Iron Springs Formation consists of sandstone and layers of conglomerate, as well as sparse thin limestone beds (see the top of the Shooting Range section in Fig. 4), which locally contain intraformational rip-up clasts.

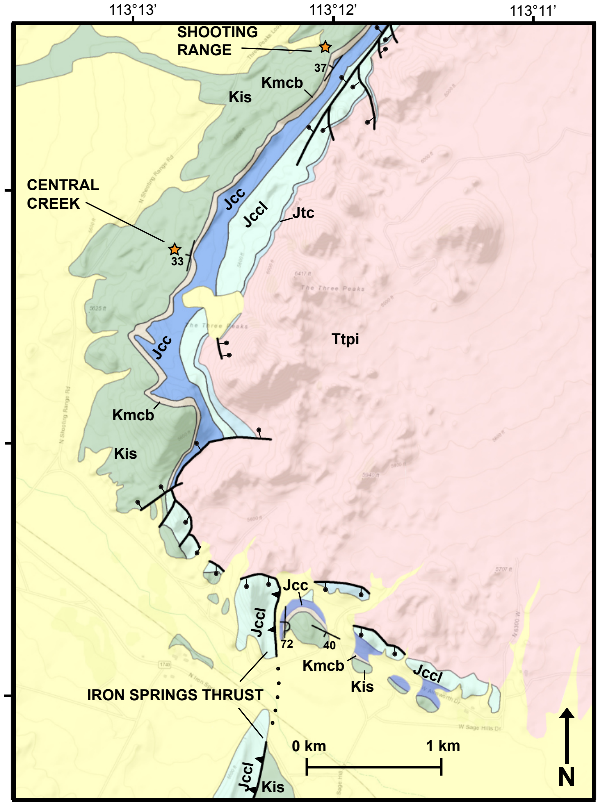

Figure 2. Geologic map of the Three Peaks area compiled from Mackin et al., 1976, and Mackin and Rowley, 1976, showing the location of the 'Central Creek' and 'Shooting Range' measured stratigraphic sections (stars). Rocks of the Co-op Creek Limestone Member of the Carmel Formation crop out in the hanging wall of the Iron Springs thrust (Knudsen and Biek, 2014). Notice also that the Iron Springs thrust deforms the Marshall Creek breccia in the footwall of the thrust, implying that the Iron Springs thrust remained active following deposition of the breccia. The Co-op Creek Limestone Member in the hanging wall of the Iron Springs thrust is the likely source of limestone clasts in the Marshall Creek breccia. The Jcc = Jurassic Crystal Creek Member of the Carmel Formation; Jccl = Jurassic Co-op Creek Limestone Member of the Carmel Formation; Jtc = Jurassic Temple Cap Formation; Kis = Cretaceous Iron Springs Formation; Kmcb = Cretaceous Marshall Creek breccia; Q = Quaternary deposits; Ttpi = Tertiary Three Peaks intrusions. Topographic basemap underlay was created using ArcGIS® software by Esri®. ArcGIS® and ArcMap™ are the intellectual property of Esri, and are used herein under license (see www.esri.com).

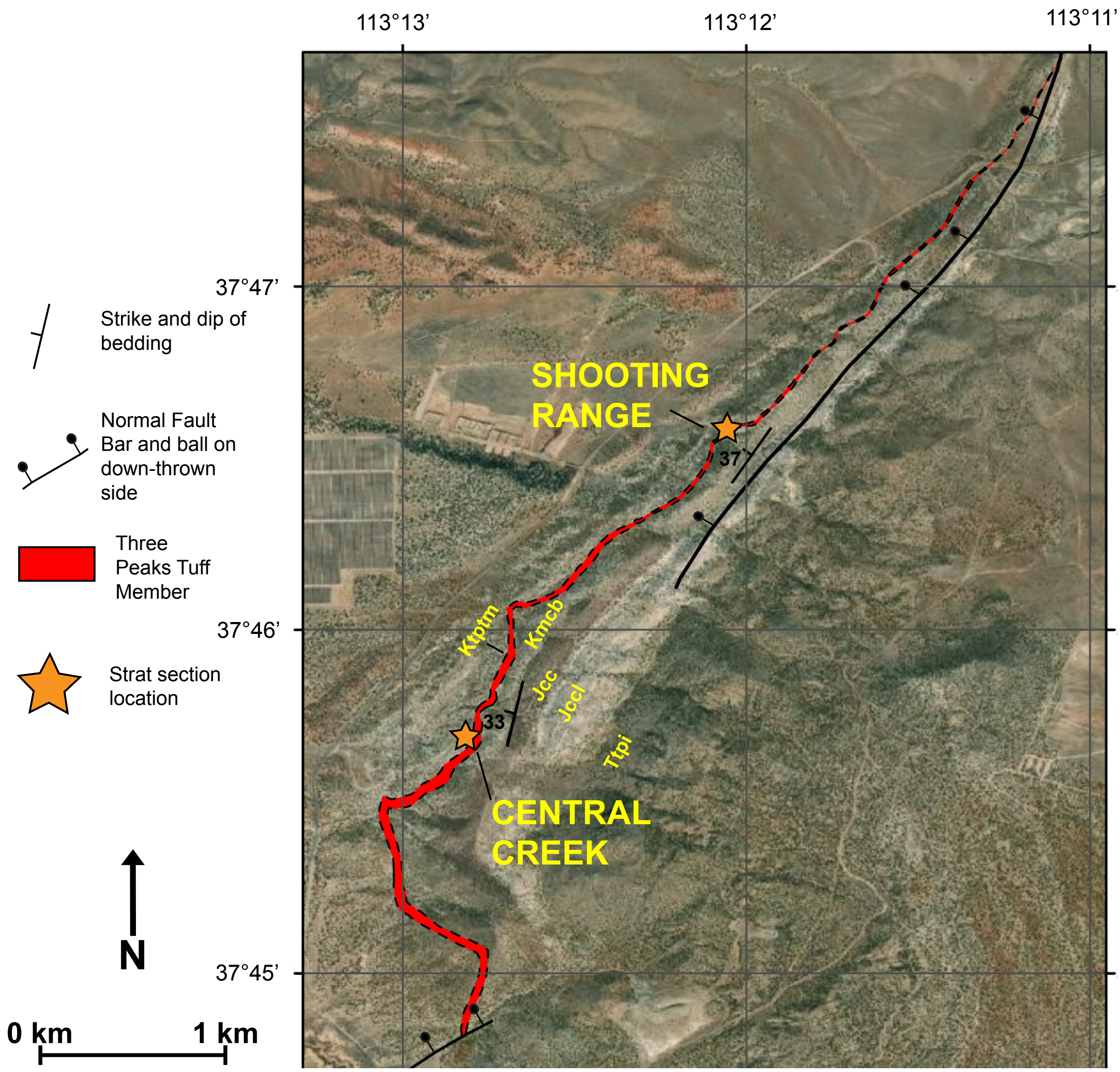

Figure 3. Simplified geologic map highlighting the outcrop distribution (in red) of the Three Peaks Tuff Member (Ktptm). Location of measured stratigraphic sections (see Fig. 4) shown as stars. Selected geologic units shown (see Fig. 2 for location of contacts) include the Marshall Creek breccia (Kmcb); the Crystal Creek Member (Jcc) and the Co-op Creek Limestone Member (Jccl) of the Carmel Formation; and the quartz monzonite of the Tertiary Three Peaks intrusions (Ttpi). Selected faults from Mackin et al. (1976) and Mackin and Rowley (1976). Aerial photo basemap underlay was created using ArcGIS® software by Esri®. ArcGIS® and ArcMap™ are the intellectual property of Esri and are used herein under license (see www.esri.com).

THE THREE PEAKS TUFF MEMBER

Description of the Three Peaks Tuff Member

We propose the name "Three Peaks Tuff Member of the Iron Springs Formation," and a type section (Figs. 2–4; Data Supplement [DS] 1; DS Table 1) for an "air-fall" tuff locally present in the stratigraphic section above the Marshall Creek breccia. Following Schmid (1981), the Three Peaks Tuff is a purple to whitish gray dacite vitric-crystal coarse ash-lapilli tuff. It is mappable along strike over several kilometers, and consists of multiple discrete beds that crop out over a stratigraphic interval of ~17 m (Figs. 2–4). Accretionary lapilli and biotite phenocrysts are conspicuous in several beds that crop out, in hand samples, and in thin sections (Fig. 6). Other phenocrysts include quartz, plagioclase, and iron oxides. Quartz and plagioclase phenocrysts are typically < 0.6 mm, and inconspicuous in hand sample. Altered glass shards are common.

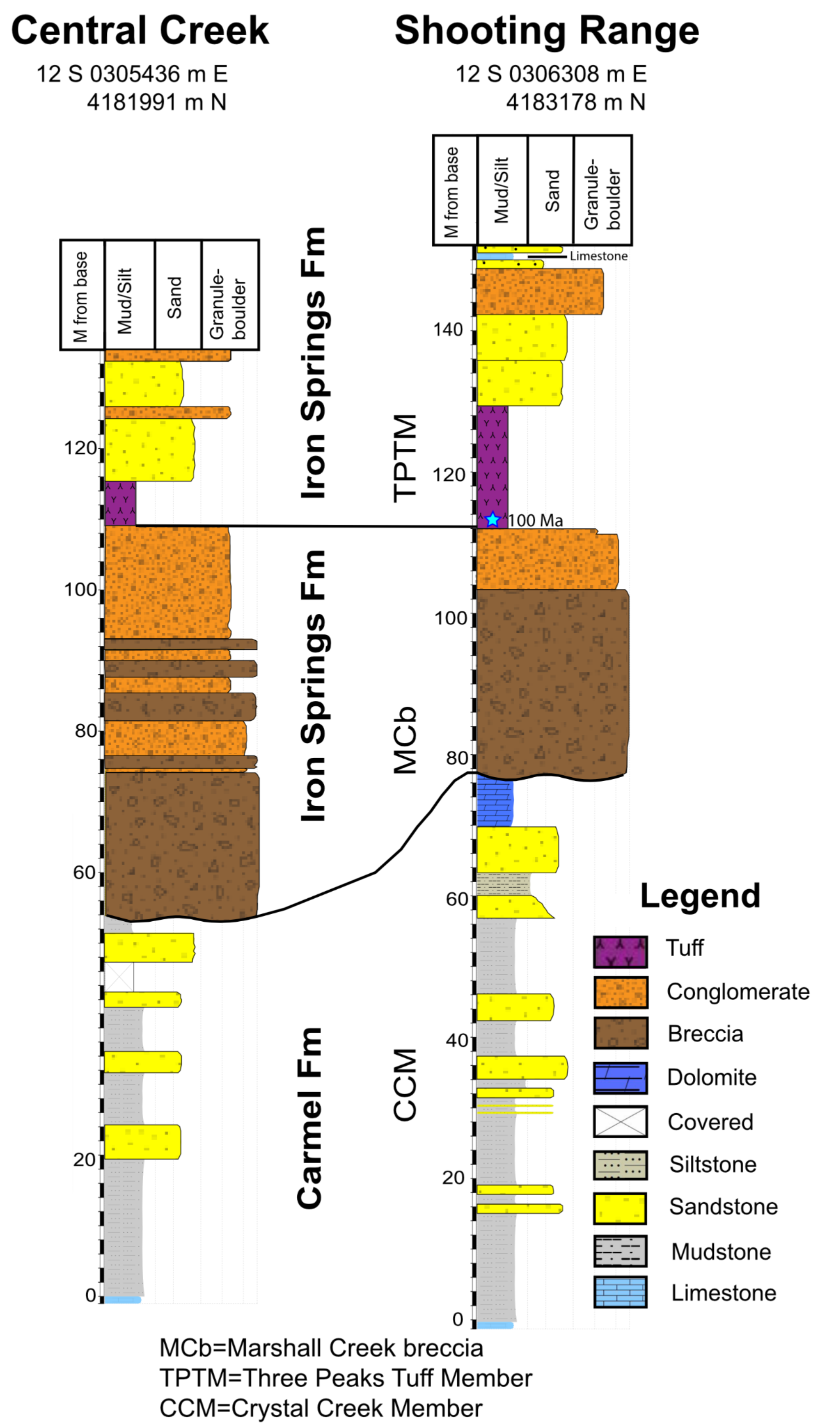

Figure 4. The 'Central Creek' and 'Shooting Range' stratigraphic columns, generated using Stratigraphic Data Analysis in R (SDAR; Ortiz et al., 2018) from the western flank of the Three Peaks (Figs. 2 and 3). Locally, the Iron Springs Formation is more than 900 m thick (Mackin, 1947; Mackin et al., 1976), and only the lowermost part of the formation was measured and shown here. A thin bed of limestone in the Iron Springs Formation crops out near the top of the Shooting Range section. Geochronology sample of the Three Peaks Tuff Member (TPTM) marked with a blue star. The high relief, sub-Cretaceous unconformity on the Crystal Creek Member (CCM) of the Jurassic Carmel Formation is marked by a wavy line. Note the interfingering of the Marshall Creek breccia (MCb) and basal conglomerate of the Iron Springs Formation in the Central Creek measured section.

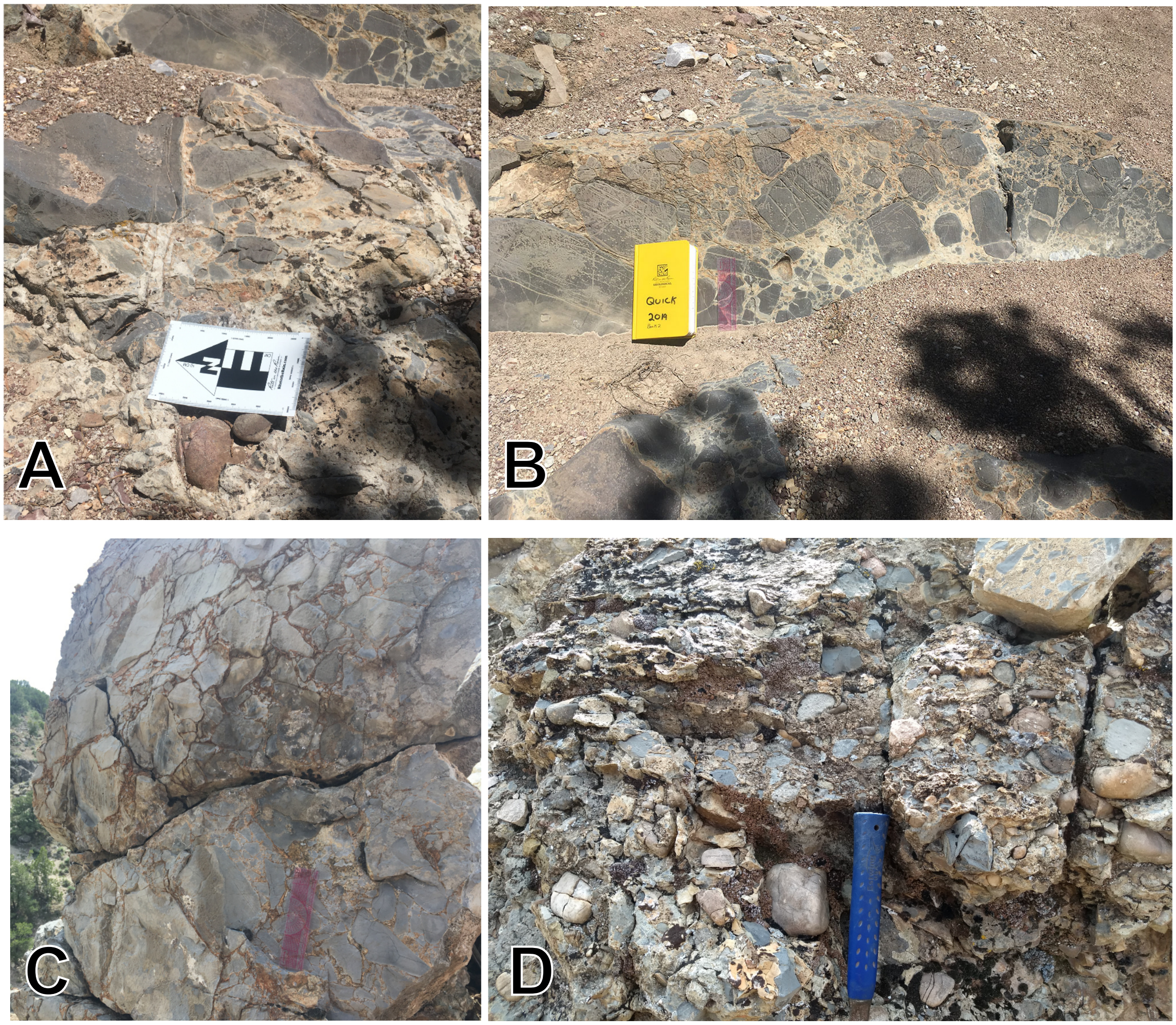

Figure 5. ***A*****,** Outcrop of the Marshall Creek breccia showing well-rounded quartzite clasts just below the scale. ***B*****,** Outcrop of the Marshall Creek breccia. Note that the gray limestone clasts are generally large and angular, and here matrix-supported in a brown lime-silt. Sparse rounded limestone clasts are present. ***C*****,** Outcrop of poorly sorted rocks of the Marshall Creek breccia with abundant angular clasts. ***D*****,** Outcrop of conglomerate of the Iron Springs Formation. Note the dark gray limestone clasts.

Sparse lithic quartzite fragments > 0.5 mm occur near the base of the tuff, and were likely locally derived during emplacement. The uppermost ash bed has been reworked, consistent with emplacement during active sediment deposition. Four samples of the tuff, analyzed for whole-rock geochemistry, plot unambiguously as dacite with trace-element signatures consistent with a volcanic arc setting (Fig. 7; DS Tables 2 and 3).

Geochronology

Zircons from the base of the tuff were dated by laser ablation-inductively coupled plasma-mass spectrometry (LA-ICP-MS) and chemical abrasion-thermal ionization mass spectrometry (CA-TIMS). Details of the methods used and the analytical results are presented in DS 2 and DS Tables 4–6. These zircons are euhedral to subhedral with euhedral to subhedral cores (Fig. 8). Zircons with anhedral cores are rare. Concentric oscillatory zoning is common, though simple, broad, patchy, and sector zoning were noted. Forty-seven zircons analyzed by LA-ICP-MS yield dates between 104.7 ± 4.0 Ma and 92.6 ± 2.4 Ma (DS Table 6). Thirty-nine of these analyses have a weighted mean date of 99.4 ± 0.8 Ma (MSWD = 0.9; probability of fit = 0.57). Of these, six zircons were analyzed by CA-TIMS. The four

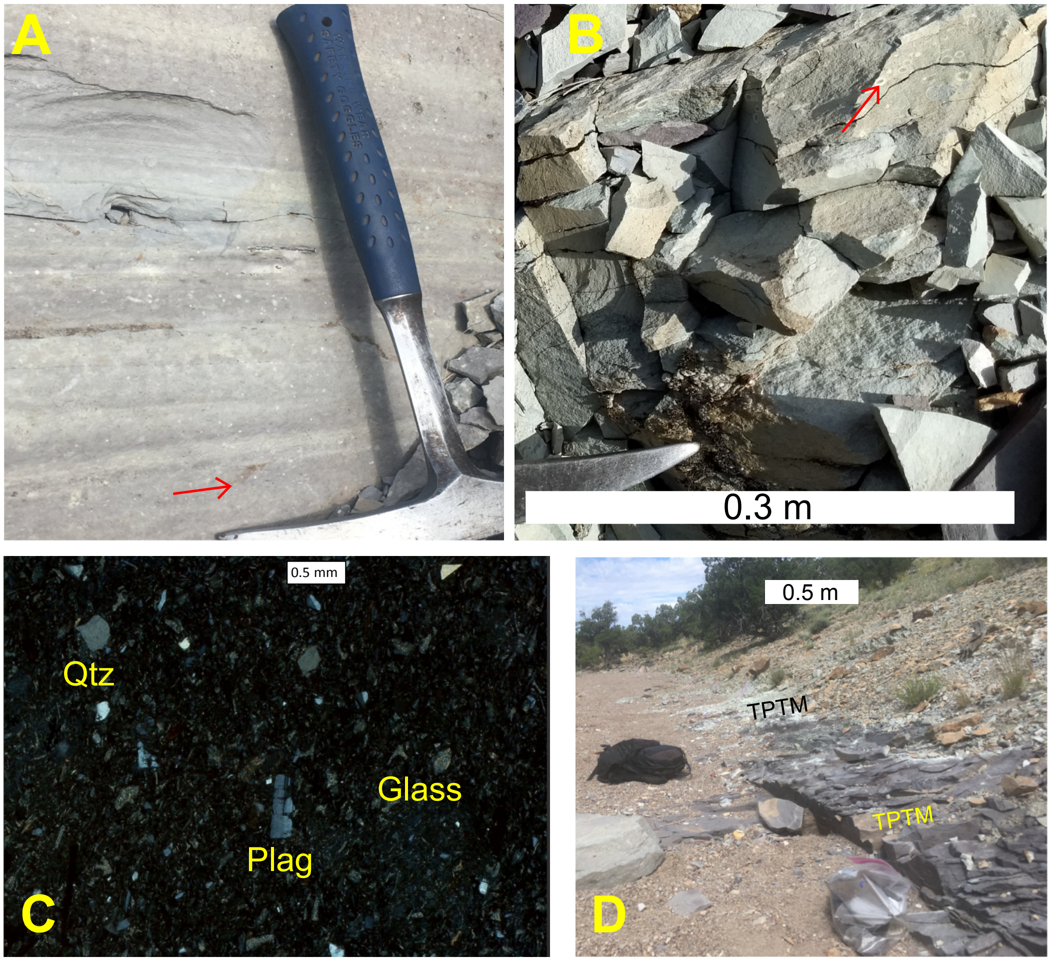

Figure 6. ***A*,** Outcrop of the Three Peaks Tuff Member (TPTM). Red arrow points to accretionary lapilli. ***B*,** Outcrop of the TPTM. Red arrow points to accretionary lapilli. ***C*,** Photomicrograph of the TPTM showing altered glass shards as well as small plagioclase (Plag) and quartz (Qtz) grains. ***D*,** An outcrop of the TPTM showing some of the color variability. Note both the purple (foreground) and white (center) beds.

youngest yield a weighted mean date of 100.18 ± 0.04 Ma (Fig. 8; DS Table 5); the other two are slightly older (100.30 ± 0.07 Ma and 100.43 ± 0.07 Ma), and may reflect older cores. We interpret the CA-TIMS date of 100.18 ± 0.04 Ma as the crystallization age for the zircons in the Three Peaks Tuff Member, providing a minimum depositional age for the Marshall Creek breccia and the Iron Springs Formation.

DISCUSSION

Tectonic Implications of Stratigraphic Relationships

Field relationships demonstrate that the Marshall Creek breccia and the Three Peaks Tuff Member are part of the lower Iron Springs Formation (Figs. 2–4). The large angular clasts of the Marshall Creek breccia (Fig. 5) originated as talus blocks transported short distances by debris flows, possibly as part of a fanglomerate and alluvial fan system (e.g., Laird and Hope, 1968; Ribes et al., 2019). The limestone of the Co-op Creek Limestone Member of the Carmel Formation and limestone clasts of the Marshall Creek breccia are indistinguishable in hand sample (see also Mackin, 1947; Mackin and Rowley, 1976; Fillmore, 1991). We suspect that the talus was derived from the Co-op Creek Limestone as it was uplifted in the hanging wall of the emergent Iron Springs thrust at the southernmost extent of the breccia (see Mackin et al., 1976; Knudsen and Biek, 2014). Between debris flow events, sediment was supplied to the alluvial system by streams carrying quartzite and limestone eroded from bedrock uplifted by the Wah Wah thrust (Fillmore, 1991). Thus, the 100.18 ± 0.04 Ma U–Pb zircon crystallization age for the Three Peaks Tuff (Fig. 8) locally

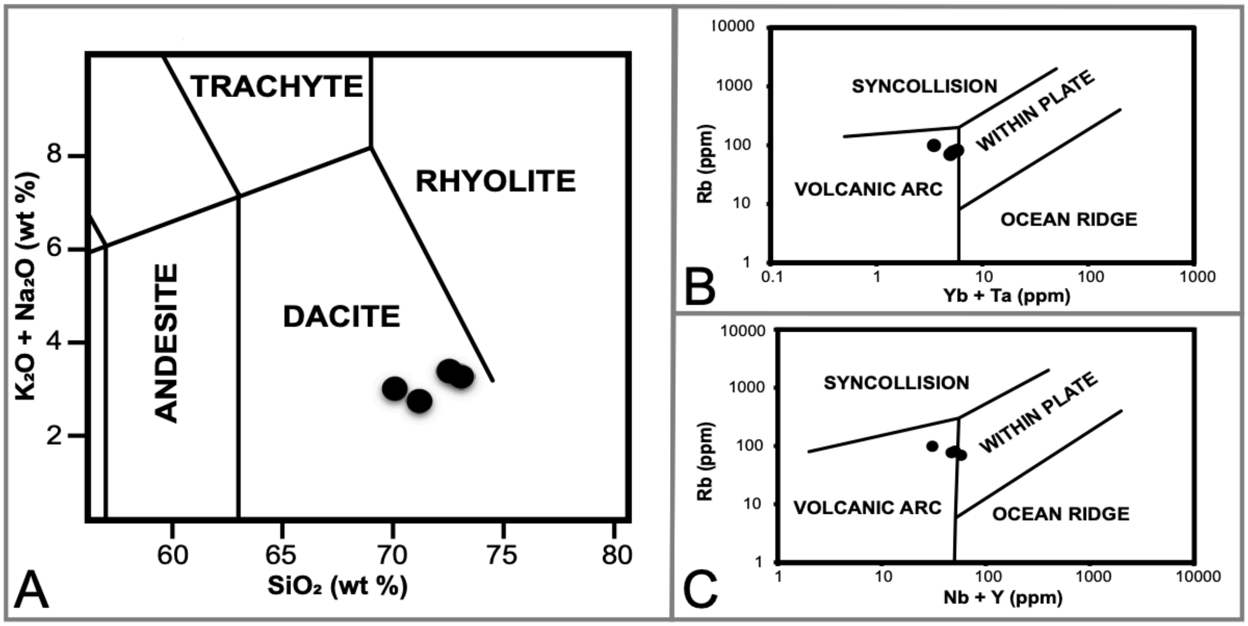

Figure 7. ***A,*** Total alkalis vs. SiO_2 diagram for whole-rock samples of the Three Peaks Tuff Member (TPTM). ***B–C,*** Trace-element discrimination diagrams (after Pearce et al., 1984) for the TPTM. Nb = niobium; Rb = rubidium; Ta = tantalum; Y = yttrium; Yb = ytterbium.

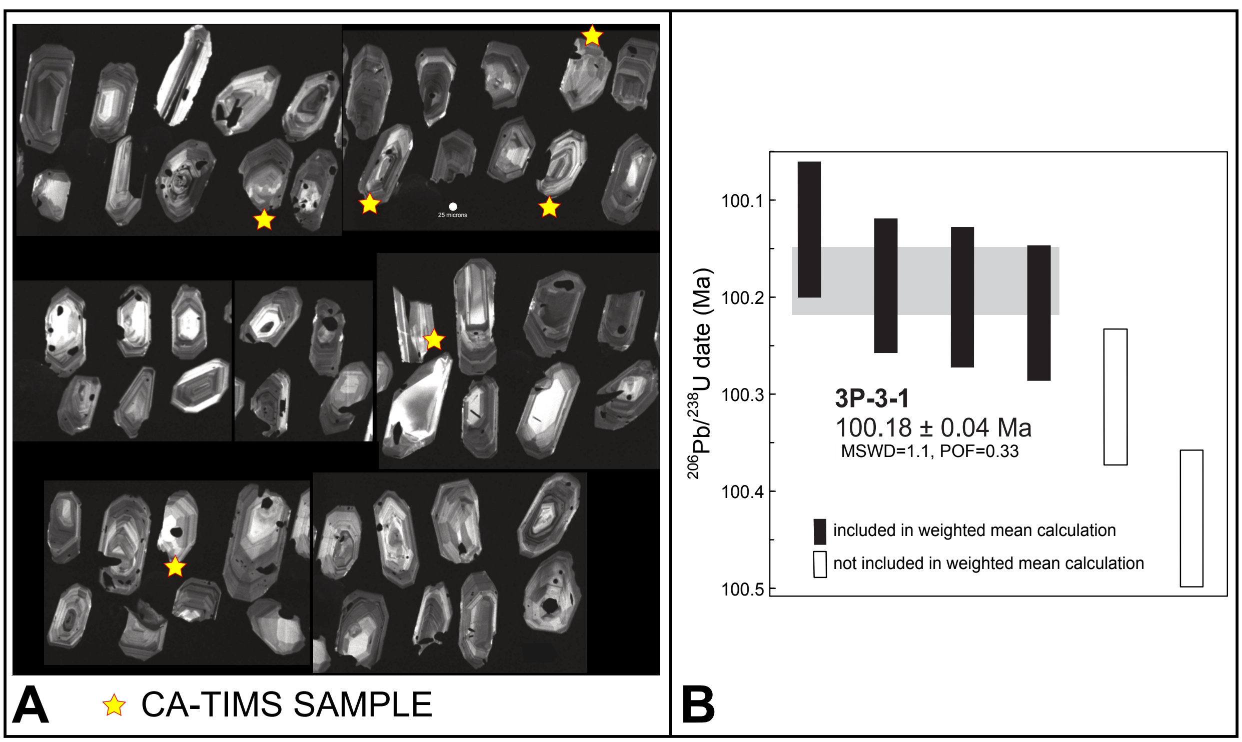

Figure 8. ***A,*** Cathodoluminescence images of zircons from sample 3P-3-1 of the Three Peaks Tuff Member. ***B,*** $^{206}Pb/^{238}U$ dates (with error) from chemical abrasion-thermal ionization mass spectrometry (CA-TIMS) analysis of zircons from sample 3P-3-1. MSWD = mean square weighted deviation; POF = probability of fit. See Data Supplement 2, Methods, for details.

constrains the depositional age of the lower Iron Springs Formation and the end of the hiatus represented by the regional sub-Cretaceous unconformity (Fig. 4) to the latest Albian–earliest Cenomanian. This age also constrains timing of early deformation on the Iron Springs thrust in proximity to the eastern leading edge of the Sevier fold-and-thrust belt in the critical intervening area between the northern and southern deformation belts (Fig. 1).

The Role of Structural Inheritance

The sinuous trace of the Sevier fold-and-thrust belt parallels the Cordilleran hingeline, which marks the western edge of thicker Precambrian crust least affected by continental rifting (Fig. 1). The location of embayments and promontories along the continental margin controls the development of salients and recesses in the orogen, a process known as "tectonic inheritance" (e.g., Thomas, 1977, 2005). At the latitude of Las Vegas (~36° N), thin-skinned deformation of the Sevier fold-and-thrust belt was of shorter duration (ca. 50 m.y.), formed a narrower deformation belt (~100 km wide), and mirrors the Cordilleran hingeline, which is located < 20 km west of the leading-edge Sevier structures. Palinspastic reconstruction, to account for basin-and-range extension (Wernicke et al., 1988), places leading-edge Sevier structures much closer to the Cordilleran hingeline (~8 km) prior to extension. We suggest the name Las Vegas *recess* for this portion of the Sevier fold-and-thrust belt that mirrors the promontory of thicker Precambrian craton, which impeded eastward thrust propagation sooner (e.g., ~99-Ma Keystone thrust) than farther to the north (Fig. 1). In contrast, the Salt Lake *salient* of the Sevier fold-and-thrust belt mirrors the presence of an embayment in the thicker Precambrian craton. Here, thin-skin thrusting was facilitated by the presence of a thinner, extended, continental crust projecting farther east into the craton ~50 km east of the Cordilleran hingeline. At this latitude (~41° N), the Sevier fold-and-thrust belt remained active longer (ca. 100 m.y.) and over a wider deformation belt (~500 km), and it propagated farther inland (e.g., 56 Ma Hogsback thrust [HBT]; Fig. 1). In addition, between the Las Vegas recess and Salt Lake salient are four "northeast–southwest-trending lineaments" (Fig. 1). These features are interpreted to be transform faults that offset the Precambrian craton (Picha and Gibson, 1985). Where these lineaments abut mid-Cretaceous thrusts (e.g., Paragonah lineaments abut the Iron Springs thrust, and Leamington lineament abuts the Charleston-Nebo thrust system), eastward thrust propagation appears to have been mostly arrested. Thus, as suggested by Picha and Gibson (1985) and Picha (1986), the role of tectonic inheritance in affecting the development of the eastern leading edge of the Sevier fold-and-thrust belt appears to involve the location of thinned continental lithosphere along the rifted margin as well as the location of strike-slip transfer zones between the continental rifts.

Alternatively, fold-and-thrust belt development may be controlled by variation in stratigraphy and sediment thickness (e.g., Chapman and DeCelles, 2015). Extreme variation in pre-deformation sediment thickness can preclude and arrest thrust-fault propagation, leading to the formation of recesses (e.g., Paulsen and Marshak, 1999). Along hingeline variation in pre-orogenic sediment thickness has been invoked as an explanation for the spatial correlation of the leading edge of the Sevier fold-and-thrust belt being arrested in the south at the latitude of Las Vegas, whereas Sevier thrusts propagate across the hingeline to the north at the latitude of Salt Lake City (Giallorenzo et al., 2018). The two hypotheses, tectonic inheritance and sediment thickness, are intimately related as the form of rifted margins can exert a high level of control on pre-orogenic sedimentation patterns. Thus, variation along the Sevier fold-and-thrust belt (i.e., Las Vegas recess and Salt Lake salient) may reflect the form of the rifted Precambrian continental margin (i.e., tectonic inheritance) as defined by the Cordilleran hingeline (e.g., Picha, 1986; Fig. 1 this paper), but the Cordilleran hingeline also marks a distinct and abrupt change in sediment thickness (Giles et al., 1999).

Evidence for Widespread Mid-Cretaceous Thrusting: Tectonic Implications

Orogenic events are defined by the linked processes of magmatism, metamorphism, and crustal deformation such that changes in one affects the others (e.g., DeCelles et al., 2009; DeCelles and Graham, 2015; Ducea et al., 2015). The mid-Cretaceous age and volcanic arc trace element signature of the Three Peaks Tuff Member (Figs. 7 and 8) associate it with the North American Cordillera magmatic flare-up at 105 to 90 Ma (Fig. 9). The mid-Cretaceous was also a time of extensive penecontemporaneous and widespread thrust-fault propagation, movement, and deformation in the Sevier orogen (Fig. 9). South of the Iron Springs thrust, at the latitude of Las Vegas, synorogenic strata constrain early movement on the Keystone thrust system to 99 Ma (Fleck and Carr, 1990). North of the Iron Springs thrust, a period of rapid cooling at 100 Ma recorded for the Pavant and Charleston-Nebo thrust sheets is interpreted to represent rapid exhumation and emplacement of the thrusts (Pujols et al., 2020). Yonkee et al. (2019) suggest the shortening rate on the Willard thrust, also in northern Utah, increased three-fold at 105 Ma. Di Fiori et al. (2020) reported deformation around 100 Ma in the central Nevada fold-and-thrust belt as constrained by the deposition age of the syncontractional Newark Canyon Formation. Early movement on the Iron Springs thrust was, therefore, synchronous with movement on the Keystone thrust to the south,

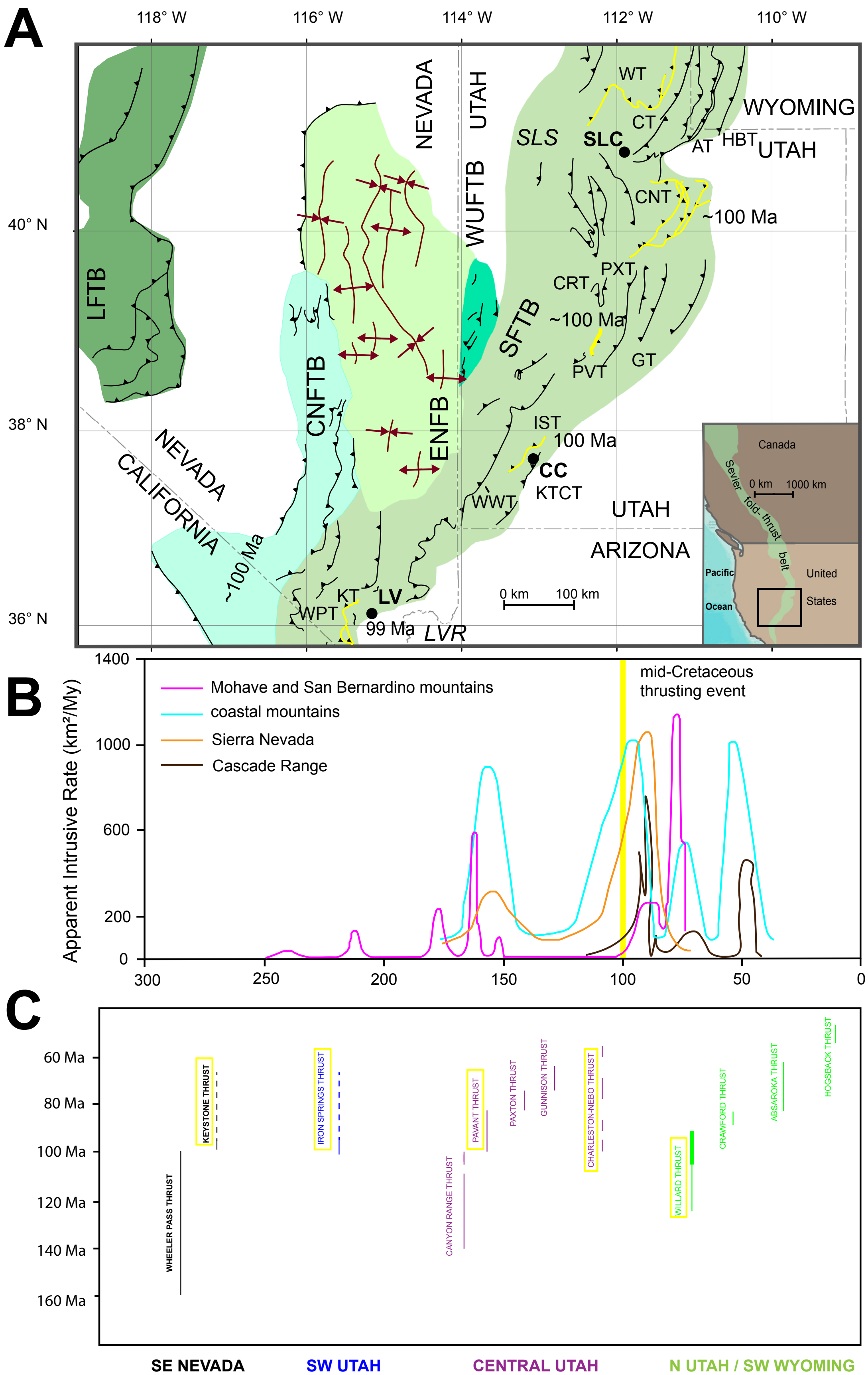
A
118° W
116° W
114° W
112° W
110° W
40° N
38° N
36° N
NEVADA
UTAH
WYOMING
UTAH
WT
CT
SLS
SLC
AT
HBT
CNT
~100 Ma
WUFTB
LFTB
CRT
PXT
~100 Ma
SFTB
PVT
GT
CNFTB
ENFB
IST
100 Ma
CC
KTCT
WWT
UTAH
ARIZONA
NEVADA
CALIFORNIA
~100 Ma
KT
LV
WPT
99 Ma
LVR
0 km
100 km
Canada
Sevier fold- thrust belt
0 km
1000 km
Pacific
Ocean
United
States
B
Apparent Intrusive Rate (km²/My)
1400
1000
600
200
0
300
250
200
150
100
50
0
Mohave and San Bernardino mountains
coastal mountains
Sierra Nevada
Cascade Range
mid-Cretaceous
thrusting event
C
60 Ma
80 Ma
100 Ma
120 Ma
140 Ma
160 Ma
WHEELER PASS THRUST
KEYSTONE THRUST
IRON SPRINGS THRUST
CANYON RANGE THRUST
PAVANT THRUST
PAXTON THRUST
GUNNISON THRUST
CHARLESTON-NEBO THRUST
WILLARD THRUST
CRAWFORD THRUST
ABSAROKA THRUST
HOGSBACK THRUST
SE NEVADA
SW UTAH
CENTRAL UTAH
N UTAH / SW WYOMING

Figure 9, previous page. ***A*,** Overview map showing key thrusts from the mid-Cretaceous thrusting event (in yellow). Some temporal constraints for the development of the Cordilleran orogen, as cited in the text, are also shown on the map. AT = Absaroka thrust; CC = Cedar City; CNFTB = central Nevada fold-and-thrust belt; CNT = Charleston-Nebo thrust; CRT = Canyon Range thrust; CT = Crawford thrust; ENFB = eastern Nevada fold belt; GT = Gunnison thrust; HBT = Hogsback thrust; IST = Iron Springs thrust; KT = Keystone thrust; KTCT = Kanarra fold and Kanarra-Taylor Creek thrust system; LFTB = Luning-Fencemaker fold-and-thrust belt; LV = Las Vegas; LVR = Las Vegas recess; PVT = Pavant thrust; PXT = Paxton thrust; SFTB = Sevier fold-and-thrust belt; SLC = Salt Lake City; SLS = Salt Lake salient; WPT = Wheeler Pass thrust; WT = Willard thrust; WUFTB = western Utah fold-and-thrust belt; WWT = Wah Wah thrust. Map compiled from Stokes et al., (1963), Picha and Gibson (1985), Willis (1999), Wyld et al., (2003), Page et al. (2005), Long (2015), Yonkee and Weil (2015), Herring and Greene (2016), and Giallorenzo et al. (2018). ***B*,** History of Cordilleran magmatism, with flare-up events represented as high points. Modified from Ducea et al. (2015). The timing of the mid-Cretaceous thrusting event is shown as a thick yellow line. **C,** Event chart for along-strike Sevier thrusting. Yellow boxes are around the names of mid-Cretaceous thrusts. The period of rapid shortening along the Willard thrust is represented as a thicker green line. Compiled from Fleck and Carr (1990), DeCelles (1994), DeCelles and Coogan, (2006), Giallorenzo et al., (2018), Yonkee et al., (2019), and Pujols et al., (2020).

and the Willard thrust and Pavant and Charleston-Nebo thrust systems to the north, as well as with deformation in the central Nevada fold-and-thrust belt in the western part of the orogen (Fig. 9A, C).

A close temporal correspondence between magmatic flare-ups and regional contractional stress regimes that lead to horizontal shortening and vertical thickening of the crust are well documented (e.g., DeCelles et al., 2009; see also Fig. 9 this paper), and imply a process-related relationship between thrusting and magmatism. Several models have been proposed as triggers for magmatic flare-ups. They vary as to the role of the driving processes operating in the lithosphere or in the convecting mantle wedge and the extent to which the processes are coupled or decoupled to the subducting slab (see Ducea et al., 2015). Thus, several sources for magmas produced during flare-ups (decoupled from the subducting slab) have been proposed. These include mid- to lower-crustal materials that undergo dehydration melting as a result of lithospheric thickening due to trench-side subduction erosion combined with retroarc shortening in foreland fold-and-thrust belts (Ducea and Barton, 2007; DeCelles et al., 2009). Alternatively, they may be derived by tectonic underplating of material scraped off the upper portion of subducted oceanic lithosphere (Clift and Vannucchi, 2004; Chapman et al., 2012). Other models for magmatic flare-ups, more closely coupled to the subducting oceanic lithosphere, include slab roll-back (Ferrari et al., 2007) or repeated injection of basaltic melts, derived from partial melting of the overlying mantle wedge, into the base of the lithosphere beneath the arc (Dufek and Bergantz, 2005). Enhanced melt-production in the mantle wedge, leading to a greater influx of basaltic magma into the lower lithosphere, is a plausible trigger for magmatic flare-ups. This process is promoted by increasing the volatile component in the melt-production zone through incorporation of subducted sediments into the mantle (Hacker et al., 2011) or higher convergence rates leading to recycling more altered, hydrated, oceanic lithosphere into the mantle (Cagnioncle et al., 2007).

Four world-wide global flare-ups, where magmatic arcs from multiple unrelated geologic provinces appear to have simultaneously produced voluminous amounts of magma in a restricted period (~30–20), are recognized (Ducea et al., 2015). One of these global magmatic flare-up events is the mid- to late-Cretaceous event (Fig. 9B). Matthews et al. (2012) documents this time as a period of "global plate reorganization," wherein plate motions were dramatically altered worldwide, possibly due to cessation of subduction in eastern Gondwana after ca. 150 m.y. of plate convergence. Ducea et al. (2015) proposed that increased production of oceanic crust at mid-oceanic ridges during this same time period led to increased rates of recycling of older oceanic lithosphere as a possible trigger for the global mid-Cretaceous magmatic flare-up. We speculate that the global plate reorganization (Matthews et al., 2012) resulted in a significant increase in the rate of plate convergence along western North America, leading to the flare-up in Cordilleran arc magmatism, and widespread thrusting at ~100 Ma (Fig. 9). Increased convergence and subduction of hydrated oceanic lithosphere would deliver volatiles to the mantle at an increased rate facilitating prolific production of basaltic magma by partial melting of the overlying, convecting, mantle wedge (Stern, 2002; Cagnioncle et al., 2007; Ardila et al., 2019). This, in turn, would promote partial melting of the lower crust (e.g., Dufek and Bergantz, 2005). This high magma flux rate, advecting heat and material into the lithosphere, resulted in an increased surface elevation of the arc, forcing the wedge taper into a supercritical condition, as the flare-up approached its peak. This, along with a presumably higher regional tectonic horizontal compressive stress, resulted in rapid eastward propagation of thrusting (e.g., the mid-Cretaceous thrusting event; see Fig. 9) across the Sevier deformation belt (see also Lageson et al., 2001; DeCelles and Graham, 2015).

CONCLUSIONS

The newly named Three Peaks Tuff Member is a dacite ash-fall tuff that is syndepositional with the lowermost Iron Springs Formation, which includes the syntectonic Marshall Creek breccia at its base. The concordant 100.18 ± 0.04 Ma U/Pb zircon crystallization age for the Three Peaks Tuff constrains the end of the regional sub-Cretaceous hiatus, and the emergence of the eastern leading edge of the Sevier fold-and-thrust belt in southwestern Utah to latest Albian–earliest Cenomanian. Along-strike variation in the spatial and temporal evolution of the Sevier fold-and-thrust belt front is, to a large extent, inherited from the structure of the rifted Precambrian crustal margin of western North America. Increased subduction rates during the mid-Cretaceous plate reorganization event likely contributed to an ~100 Ma magmatic flare-up, which is linked to the widespread mid-Cretaceous shortening across the orogen, as indicated both by the Three Peaks Tuff Member and the Iron Springs thrust, and by other synchronous thrusts in the Sevier fold-and-thrust belt. Defining the nature of feed-back processes that may link the other magmatic flare-ups (Fig. 9C) to episodes of punctuated accelerated deformation throughout the spatial and temporal evolution of the Sevier orogeny (e.g., ~165–150 Ma, ~60–50 Ma) is an important topic that needs to be further investigated.

ACKNOWLEDGMENTS

John P. Hogan thanks Dr. Jason Kaiser for introducing him to the geology of the Three Peaks area where this research was initiated during the Missouri University of Science and Technology (Missouri S&T) geosciences field camp. Daniel Quick acknowledges support from the Missouri S&T Department of Geosciences, Geological Engineering, and Petroleum Engineering, the Alfred Spreng Graduate Research Award, William Chandonia for assistance with fieldwork, and Edward Duarte Martinez for assistance with Stratigraphic Analysis Data in R (SDAR). This manuscript benefited from the constructive reviews of David C. Greene, an anonymous reviewer, and *Rocky Mountain Geology* (*RMG*) Science Co-Editors Arthur Snoke and Ron Frost. In addition, many thanks are extended to *RMG* Managing Editor Brendon Orr and Technical Copy Editor Robert Waggener for their highly professional editorial assistance.

REFERENCES CITED

Ardila, A.M.M., Paterson, S.R., Memeti, V., Parada, M.A., and Molina, P.G., 2019, Mantle driven Cretaceous flare-ups in Cordilleran arcs: Lithos, v. 326–327, p. 19–27, https://doi: 10.1016/j.lithos.2018.12.007.

Barker, D.S., 1995, Crystallization and alteration of quartz monzonite, Iron Springs mining district, Utah: Relation to associated iron deposits: Economic Geology, v. 90, p. 2,197–2,217.

Cagnioncle, A-M., Parmentier, E.M., and Elkins-Tanton, L.T., 2007, Effect of solid flow above a subducting slab on water distribution and melting at convergent plate boundaries: Journal of Geophysical Research: Solid Earth, v. 112, B09402.

Chandonia, W., Hogan, J.P., and Eckert, A., 2018, "Rollover-break thrusts" and advancement of the leading edge of the Sevier fold and thrust belt, southwest Utah: Geological Society of America Abstracts with Programs, v. 50, no. 6.

Chapman, A.D., Saleeby, J.B., Wood, D.J., and four others, 2012, Late Cretaceous gravitational collapse of the southern Sierra Nevada batholith, California: Geosphere, v. 8, p. 314–341.

Chapman, J.B., and DeCelles, P.G., 2015, Foreland basin stratigraphic control on thrust belt evolution: Geology, v. 43, p. 579–582, https://doi:10.1130/G36597.1.

Clift, P., and Vannucchi, P., 2004, Controls on tectonic accretion versus erosion in subduction zones: Implications for the origin and recycling of the continental crust: Reviews of Geophysics, v. 42, RG2001, 31 p., https://doi:10.1029/2003RG000127.

DeCelles, P.G., 1994, Late Cretaceous–Paleocene synorogenic sedimentation and kinematic history of the Sevier thrust belt, northeast Utah and southwest Wyoming: Geological Society of America Bulletin, v. 106, p. 32–56, https://doi:10.1130/0016-7606(1994)106<0032:LCPSSA>2.3.CO;2.

____2004, Late Jurassic to Eocene evolution of the Cordilleran thrust belt and foreland basin systems, western USA: American Journal of Science, v. 304, p. 105–168, https://doi:10.2475/ajs.304.2.105.

DeCelles, P.G., and Coogan, J.C., 2006, Regional structure and kinematic history of the Sevier fold-and-thrust belt, central Utah: Geological Society of America Bulletin, v. 118, p. 841–864, https://doi.org/10.1130/B25759.1.

DeCelles, P.G., and Graham, S.A., 2015, Cyclical processes in the North American Cordilleran orogenic system: Geology, v. 43, p. 499–502, https://doi:10.1130/G36482.1.

DeCelles, P.G., Ducea, M.N., Kapp, P., and Zandt, G., 2009, Cyclicity in Cordilleran orogenic systems: Nature Geoscience, v. 2, p. 251–257, https:// doi:10.1038/ngeo469.

Di Fiori, R.V., Long, S.P., Fetrow, A.C., and three others, 2020, Syncontractional deposition of the Cretaceous Newark Canyon Formation, Diamond Mountains, Nevada: Implications for strain partitioning within the

U.S. Cordillera: Geosphere, v. 16, p. 546–566, https://doi:10.1130/GES02168.1.

Ducea, M.N., and Barton, M.D., 2007, Igniting flare-up events in Cordilleran arcs: Geology, v. 35, p. 1,047–1,050.

Ducea, M.N., Paterson, S.R., and DeCelles, P.G., 2015, High-volume magmatic events in subduction systems: Elements, v. 11, p. 99–104, https://doi.org/10.2113/gselements.11.2.99.

Dufek, J., and Bergantz, G.W., 2005, Lower crustal magma genesis and preservation: a stochastic framework for the evaluation of basalt–crust interaction: Journal of Petrology, v. 46, p. 2,167–2,195.

Ferrari, L., Valencia-Moreno, M., and Bryan, S., 2007, Magmatism and tectonics of the Sierra Madre Occidental and its relation with the evolution of the western margin of North America: Geological Society of America Special Paper 442, p. 1–39.

Fillmore, R.P., 1991, Tectonic influence on sedimentation in the southern Sevier foreland, Iron Springs Formation (Upper Cretaceous), southwestern Utah, *in* Nations, J.D., and Eaton, J.G., eds., Stratigraphy, depositional environments, and sedimentary tectonics of the western margin, Cretaceous Western Interior Seaway: Geological Society of America Special Paper 260, p. 9–25.

Fleck, R.J., and Carr, M.D., 1990, The age of the Keystone thrust: Laser-fusion $^{40}Ar/^{39}Ar$ dating of foreland basin deposits, southern Spring Mountains, Nevada: Tectonics, v. 9, p. 467–476.

Friedrich, A.M., and Bartley, J.M., 2003, Three-dimensional structural reconstruction of a thrust system overprinted by postorogenic extension, Wah Wah thrust zone, southwestern Utah: Geological Society of America Bulletin, v. 115, p. 1,473–1,491, https://doi.org/10.1130/B25148.1.

Giallorenzo, M.A., Wells, M.L., Yonkee, W.A., Stockli, D.F., and Wernicke, B.P., 2018, Timing of exhumation, Wheeler Pass thrust sheet, southern Nevada and California: Late Jurassic to middle Cretaceous evolution of the southern Sevier fold-and-thrust belt: Geological Society of America Bulletin, v. 130, p. 558–579, https://doi:10.1130/B31777.1.

Giles, K.A., Bocko, M., and Lawton, T.F., 1999, Stacked Late Devonian lowstand shorelines and their relation to tectonic subsidence at the Cordilleran Hingeline, western Utah: Journal of Sedimentary Research, v. 69, p. 1,181–1,190, https://doi:10.2110/jsr.69.1181.

Greene, D.C., 2014, The Confusion Range, west-central Utah: Fold-thrust deformation and a western Utah thrust belt in the Sevier hinterland: Geosphere, v. 10, p. 148–169, https://doi:10.1130/GES00972.1.

Hacker, B.R., Kelemen, P.B., and Behn, M.D., 2011, Differentiation of the continental crust by relamination: Earth and Planetary Science Letters, v. 307, p. 501–516.

Herring, D.M., and Greene, D.C., 2016, The western Utah thrust belt in the larger context of the Sevier orogeny, *in* Comer, J.B., Inkenbrandt, P.C., Krahulec, K.A., and Pinnell, M.L., eds., Resources and geology of Utah's West Desert: Utah Geological Association Publication 45, p. 131–146.

Knudsen, T.R., and Biek, R.F., 2014, Interim geologic map of the Cedar City NW quadrangle, Iron County, Utah: Utah Geological Survey Open-File Report 627, scale 1:24,000, 2 sheets, 18 p. text.

Lageson, D.R., Schmitt, J.G., Horton, B.K., Kalakay, T.J., and Burton, B.R., 2001, Influence of Late Cretaceous magmatism on the Sevier orogenic wedge, western Montana: Geology, v. 29, p. 723–726.

Laird, M.G., and Hope, J.M., 1968, The Torea Breccia and the Papahaua overfold: New Zealand Journal of Geology and Geophysics, v. 11, p. 418–434, https://doi:10.1080/00288306.1968.10423660.

Long, S.P., 2015, An upper-crustal fold province in the hinterland of the Sevier orogenic belt, eastern Nevada, U.S.A.: A Cordilleran valley and ridge in the Basin and Range: Geosphere, v. 11, p. 404–424, https://doi:10.1130/GES01102.1.

Mackin, J.H., 1947, Some structural features in the intrusions in the Iron Springs district: Guidebook to the geology of Utah, no. 2: Utah Geological Society, 62 p.

Mackin, J.H., and Rowley, P.D., 1976, Geologic map of the Three Peaks quadrangle, Iron County, Utah: U.S. Geological Survey Geologic Quadrangle Map GQ-1297, scale 1:24,000, 1 sheet.

Mackin, J.H., Nelson, W.H., and Rowley, P.D., 1976, Geologic map of the Cedar City NW quadrangle, Iron County, Utah: U.S. Geological Survey Geologic Quadrangle Map GQ-1295, scale 1:24,000, 1 sheet.

Matthews, K.J., Seton, M., and Müller, R.D., 2012, A global-scale plate reorganization event at 105–100 Ma: Earth and Planetary Science Letters, v. 355–356, p. 283–298, https://doi:10.1016/j.epsl.2012.08.023.

Ortiz, J.R., and Jaramillo, C.A., 2018, SDAR: A toolkit for stratigraphic data analysis in R: [Dataset] Distributed by Smithsonian Research Online, https://doi:10.25570/STRI/10088/35917.

Page, W.R., Lundstrom, S.C., Harris, A.G., and nine others, 2005, Geologic and geophysical maps of the Las Vegas 30′ × 60′ quadrangle, Clark and Nye counties, Nevada, and Inyo County, California: U.S. Geological Survey Scientific Investigations Map 2814, scale 1: 5,000,000, 2 sheets, 58 p. text.

Paulsen, T., and Marshak, S., 1999, Origin of the Uinta recess, Sevier fold-thrust belt, Utah: Influence of basin architecture on fold-thrust belt geometry: Tectonophysics, v. 312, p. 203–216, https://doi:10.1016/S0040-1951(99)00182-1.

Pearce, J.A., Harris, N.B.W., and Tindle, A.G., 1984, Trace element discrimination diagrams for the tectonic interpretation of granitic rocks: Journal of Petrology, v. 25, p. 956–983.

Picha, F., 1986, The influence of preexisting tectonic trends on geometries of the Sevier orogenic belt and its foreland in Utah, *in* Peterson, J.A., ed., Paleotectonics and sedimentation in the Rocky Mountain region, United States: American Association of Petroleum Geologists Memoir 41, p. 309–320.

Picha, F., and Gibson, R.I., 1985, Cordilleran hingeline: Late Precambrian rifted margin of the North American craton and its impact on the depositional and structural history, Utah and Nevada: Geology, v. 13 p. 465–468, https://doi: 10.1130/0091-7613(1985)13<465:CHLPRM>2.0.CO;2.

Pujols, E.J., Stockli, D.F., Constenius, K.N., and Horton, B.K., 2020, Thermochronological and geochronological constraints on Late Cretaceous unroofing and proximal sedimentation in the Sevier orogenic belt, Utah: Tectonics, v. 39, https://doi.org/10.1029/2019TC005794.

Ribes, C., Ghienne, J.-F., Manatschal, G., and four others, 2019, Long-lived mega fault-scarps and related breccias at distal rifted margins: Insights from present-day and fossil analogues: London, United Kingdom, Journal of the Geological Society, v. 176, p. 801–816, https://doi: 10.1144/jgs2018-181.

Schmid, R., 1981, Descriptive nomenclature and classification of pyroclastic deposits and fragments: Recommendations of the IUGS Subcommission on the Systematics of Igneous Rocks: Geology, v. 9, p. 41–43.

Stern, R.J., 2002, Subduction zones: Reviews of Geophysics, v. 40, p. 3-1-3-38, https://doi: 10.1029/2001RG000108.

Stokes, W.L., Madsen, J.H., Jr., and Hintze, L.F., 1963, Geologic map of Utah: Utah State Land Board and University of Utah, scale 1:250,000, 4 sheets.

Thomas, W.A., 1977, Evolution of Appalachian-Ouachita salients and recesses from reentrants and promontories in the continental margin: American Journal of Science, v. 277, p. 1,233–1,278.

____2005, Tectonic inheritance at a continental margin: GSA Today, v. 16, p. 4–11, https://doi: 10.1130/1052-5173(2006)016[4:TIAACM]2.0.CO;2.

Van Kooten, G.K., 1988, Structure and hydrocarbon potential beneath the Iron Springs laccolith, southwestern Utah: Geological Society of America Bulletin, v. 100, p. 1,533–1,540.

Wernicke, B., Axen, G.J., and Snow, J.K., 1988, Basin and Range extensional tectonics at the latitude of Las Vegas, Nevada: Geological Society of America Bulletin, v. 100, p. 1,738–1,757.

Willis, G.C., 1999, The Utah thrust system—an overview, *in* Spangler, L.E., and Allen, C.J., eds., Geology of northern Utah and vicinity: Utah Geological Association Publication 27, p. 1–9.

Wyld, S.J., Rogers, J.W., and Copeland, P., 2003, Metamorphic evolution of the Luning-Fencemaker fold-thrust belt, Nevada: Illite crystallinity, metamorphic petrology, and $^{40}Ar/^{39}Ar$ geochronology: The Journal of Geology, v. 111, p. 17–38, https://doi: 10.1086/344663.

Yonkee, W.A., and Weil, A.B., 2015, Tectonic evolution of the Sevier and Laramide belts within the North American Cordillera orogenic system: Earth-Science Reviews, v. 150, p. 531–593, https://doi: 10.1016/j.earscirev.2015.08.001.

Yonkee, W.A., Eleogram, B., Wells, M.L., and three others, 2019, Fault slip and exhumation history of the Willard thrust sheet, Sevier fold-thrust belt, Utah: Relations to wedge propagation, hinterland uplift, and foreland basin sedimentation: Tectonics, v. 38, p. 2,850–2,893, https://doi:10.1029/2018TC005444.

SCIENCE EDITORS: B. RONALD FROST AND ARTHUR W. SNOKE

[1]*Rocky Mountain Geology*, a list of samples collected, whole-rock-major and trace-element geochemistry, laser ablation-inductively coupled plasma-mass spectrometry (LA-ICP-MS), and chemical abrasion-thermal ionization mass spectrometry (CA-TIMS) zircon data, field photos, and geochronology methods, is available online as data supplement downloads accompanying this article.